Journal of Ceramic Processing Research. Vol. 18, No. 11, pp. 792~795 (2017)

J O U R N A L O F
Ceramic Processing Research

Influence of oxygen flow rate on optical and electrical properties of SnO_2/Ag/SnO_2 multilayer thin film deposited on flexible substrate

Tea-Keun Kim and Gun-Eik Jang*

Department of Materials Engineering, Chungbuk National University, Cheongju 28644, Korea

We investigated effect of O_2/Ar gas flow ratio on structural, optical, and electrical properties of SnO_2/Ag/SnO_2 multilayer thin films that were deposited by sequential using RF/DC magnetron sputtering at room temperature on PET substrate. As the O_2/Ar gas flow ratio increases from 0 to 1.25% in SnO_2 (35 nm)/Ag (13 nm)/SnO_2 (35 nm) multilayer film, the transmittances varied from 81.2 to 87.1% at 550 nm wavelength, whereas the sheet resistance maintained around 7 Ω/□. The highest value of figure of merit (φ_{TC}) was $35.3 \times 10^{-3}\Omega^{-1}$ for O_2/Ar flow ratio of 1%. In addition, the measured transmittance and the sheet resistance was 87.1% at 550 nm and 7.14 Ω/□, respectively.

Key words: OMO structure, Flexibility, Figure of merit, Transmittance.

Introduction

Transparent electronics is an emerging technology that employs wide bandgap semiconductors to realize invisible circuits for next generation optoelectronic devices. The rapid demand for flexible displays (FDs) of mobile electronic devices, requires the development of light-transmitting electrodes possessing both mechanical flexibility and environmental stability, in addition to good optical transparency (> 85%) in the visible region [1] and low electrical resistivity ($< 10^{-4}\,\Omega$·cm). Such broad combination of properties cannot be obtained from conventional transparent conducting oxide (TCO) materials, typically represented by indium tin oxide (ITO), which must be deposited at room-temperature on heat-sensitive polymer substrates, mainly due to their low conductivity and mechanical brittleness [2, 3].

Recently thin film-type oxide/metal/oxide (OMO) configuration, metals inserted between transparent thin oxide films exhibit favorable optoelectrical characteristics for flexible transparent conducting electrodes (FTCEs). In addition, the OMO structure ensure superior mechanical flexibility against severe substrate bending conditions [1, 3, 4], along with competitive stability under ambient atmosphere. Moreover, the high polymer flexible substrate, such as polyethylene terephalate (PET), polycarbonate (PC), polyethersulfone (PES), polyethylene naphthalate (PEN), or polyimide (PI) are used for the above flexible applications [5-8]. Many advantages of the metal embedded multilayer structure have been over the single layer of TCO. So far, a number of research projects have been undertaken to find potential alternative for ITO electrode on flexible substrates [9-15] such as pure and Mn doped SnO_2, ZnO, or ZnO doped with other metals (i.e, aluminum (Al), and gallium (Ga), etc.), Nb_2O_5, TiO_2, graphene, and carbon nanotube (CNT) sheets. However, most papers are reporting the effect of TCO and metal layer with different thickness on electrical and optical characteristics, not much by processing condition. Based on our experimental results, proper control of processing parameter, especially the gas mixture ratio between O_2 and Ar, was found to be crucial in attaining a high transmittance and improved electrical properties. In order to find the optimized processing condition in gas mixture, SnO_2/Ag/SnO_2 multilayer films were prepared on PET substrate by sequential RF/DC magnetron sputtering at room temperature. And then SnO_2/Ag/SnO_2 multilayer films has been systematically investigated the effect on optical and electrical properties as a function of the O_2/Ar gas flow ratio.

Experimental Methods

Multilayer thin films of SnO_2/Ag/SnO_2 were deposited on polyethylene terephthalate (PET) substrates at room temperature by RF and DC magnetron sputtering. The sputtering deposition parameters of SnO_2 and Ag thin were base pressure of 1.5×10^{-5} Torr and working pressure of 3.3×10^{-3}, respectively. The atmosphere was maintained at Ar flow rate of 40 sccm and the O_2 flow rate was changed from 0 to 0.5 sccm during SnO_2 deposition. Prior to experiments, thickness of each layers were optimized by Essential Macleod Program (EMP) to obtain the best optical properties. Based on

*Corresponding author:
Tel : +82-43-261-2412
Fax: +82-43-271-3222
E-mail: gejang@chungbuk.ac.kr

results of EMP simulation, the thickness of upper and lower SnO_2 layer was kept constant at 35 nm and that of embedded Ag layer was taken about 13 nm to form a continuous layer, necessary for electrical conduction. The structure and phase identification of the films was analyzed by using X-ray diffraction (XRD) with Cu Kα radiation. The optical transmittance spectrum of the tri-layer structures was estimated using UV-VIS-NIR spectrophotometer (KONICA-MINOLTA CM-3600d). The electrical properties of the films were determined by Four-Point-Probe system. The interfacial properties of SnO_2/Ag/SnO_2 thin films were analyzed using XPS depth profiling.

Results and Discussion

The XRD patterns of the SnO_2/Ag/SnO_2 multilayer films as a function of O_2/Ar gas flow ratio were shown in Fig. 1. As shown in Fig. 1, the PET diffraction peak appears strongly at 25.8 ° without any additional peaks for the film deposited with pure Ar. Even, O_2/Ar gas flow ratio is increased, especially O_2/Ar gas flow ratio reaches to 1.25%, the PET peak appears strongly, without any noticeable changes in diffraction pattern and relative intensity. Those results demonstrated that all the SnO_2/Ag/SnO_2 multilayer films deposited on PET film at room temperature exhibited the amorphous phase, regardless of O_2/Ar gas flow ratio.

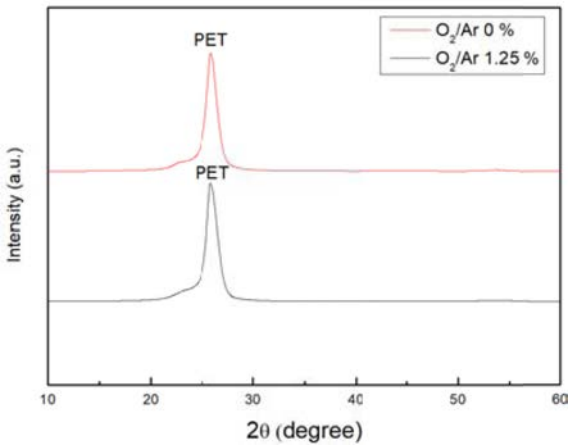

Fig. 1. XRD patterns obtained from SnO_2/Ag/SnO_2 multilayer films with O_2/Ar gas mixture ratio of 0% and 1.25%.

Fig. 2 shows the optical transmittance spectra of the SnO_2 (35 nm)/Ag (13 nm)/SnO_2 (35 nm) multilayer films on PET substrate as a function of O_2/Ar gas flow ratio at 550 nm wavelength and average of visible radiation ranges. The transmittance ranges of the all SnO_2 (35 nm)/Ag (13 nm)/SnO_2 (35 nm) tri-layered films were 81.2%-87.1% in the visible region, showing tendency of increase with increasing the O_2/Ar gas flow ratio. However, the transmittance at 550 nm wavelength was showed over 80% on the whole, the average transmittance in visible range over 80% was only in the range of O_2/Ar gas flow ratio from 0.75 to 1.25%. The maximum transmittance of 87.1% at 550 nm was observed in the SnO_2 (35 nm)/Ag (13 nm)/SnO_2 (35 nm) multilayer film deposited with 1% O_2/Ar gas flow ratio.

Fig. 3 represented the sheet resistance (R_s) and resistivity of SnO_2 (35 nm)/Ag (13 nm)/SnO_2 (35 nm) multilayer films on PET substrate as a function of O_2/Ar gas flow ratio. The sheet resistance (R_s) varied from 7.1 to 7.5 Ω/□ depending on the O_2/Ar gas flow ratio, and overall remained around 7 Ω/□. Resistivity also changed from 5.7 to 6.2 × 10^{-5} Ω·cm with different O_2/Ar gas flow ratio and the average value was around 6.0 × 10^{-5} Ω·cm. The reason of low resistive multilayer in OMO structure can be understood as amorphous thin film growth is a non-equilibrium thermodynamic process, which generate more n-type defects such as V_o and Sn_i as compared to equilibrium thermodynamic process and thus enhancing more channel for their electrical conduction. However, the electrical conduction of the OMO multilayer mainly attributed to the flow through the Ag metal layer due to its low resistivity

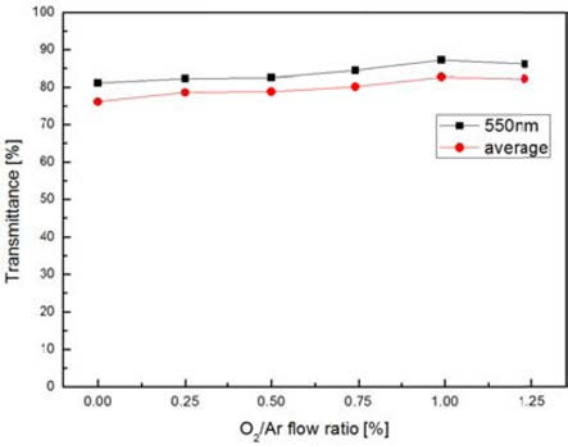

Fig. 2. The transmittance of SnO_2 (35 nm)/Ag (13 nm)/SnO_2 (35 nm) multilayer films on PET substrate as a function of O_2/Ar gas flow ratio at 550 nm wavelength in the visible radiation range.

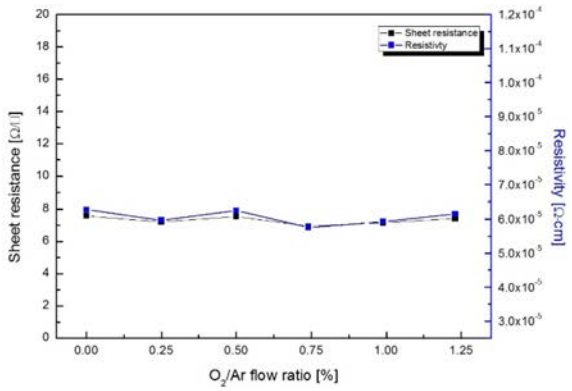

Fig. 3. The variation in sheet resistance (R_s) and resistivity of SnO_2 (35 nm)/Ag (13 nm)/SnO_2 (35 nm) multilayer films on PET substrate as a function of O_2/Ar gas flow ratio.

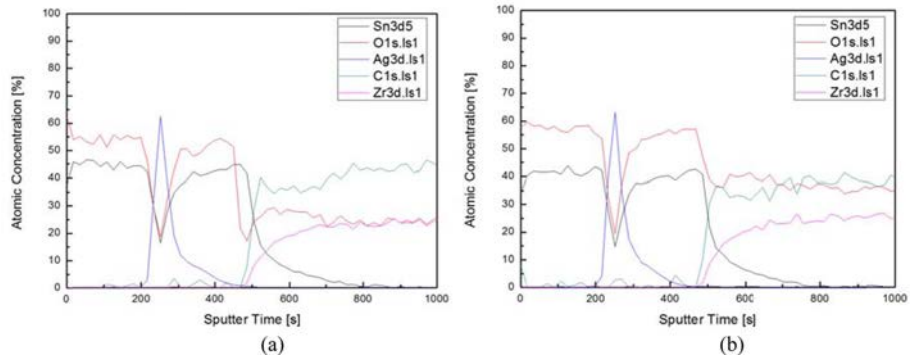

Fig. 4. XPS depth profile of SnO_2 (35 nm)/Ag (13 nm)/SnO_2 (35 nm) multilayer films on PET substrate as a function of O_2/Ar flow ratio at (a) 0% and (b) 1.25%.

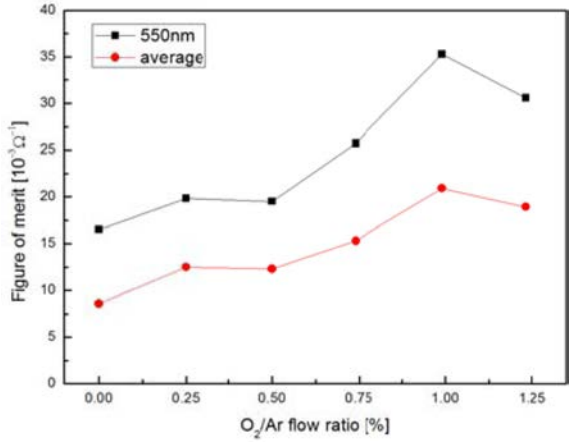

Fig. 5. The calculated figure of merit (φ_{TC}) of SnO_2 (35 nm)/Ag (13 nm)/SnO_2 (35 nm) multilayer films on PET substrate as a function of O_2/Ar gas flow ratio at 550 nm wavelength and average of visible radiation range.

[16]. Therefore, we assume that there was no noticeable influence of the Ag layer due to O_2/Ar gas flow ratio change.

Fig. 4 showed the XPS depth profile of SnO_2 (35 nm)/Ag (13 nm)/SnO_2 (35 nm) multilayer thin film on PET substrate as a function of O_2/Ar flow ratio at 0% and 1.25%. Atomic concentration average of Sn was decreased from 40.3 to 37.7%, whereas atomic concentration average of O was increased from 47.3 to 52.3% at an O_2/Ar ratio of 0 to 1.25%. From the results of Figs. 2 and 4, it can be explained that when O_2/Ar flow ratio is lower, the particles sputtered from the target cannot be oxidated enough so the prepared SnO_2 multilayer films are anoxic and sub-oxides such as SnO_x in the films. The sub-oxides resulting in the absorption and scattering in the visible spectra can be comprised possibly in the films [17]. On the other hand, as O_2/Ar flow ratio increase, the transmittance of SnO_2/Ag/SnO_2 is higher because sub-oxides can be oxidated. However, when O_2/Ar flow ratio is over high-point, the redundant oxygen can be absorbed in the defect such as grain boundary and microcrack [18]. The redundant oxygen can might cause optical absorption and scattering.

The figure of merit (FOM) is a significant factor that relates the sheet resistance and transmittance. To compare the performance of the TCO fabricated in this study, Haacke's figure of merit (FOM) of SnO_2/Ag/SnO_2 multilayer film was plotted as a function of O_2/Ar gas flow ratio. FOM (φ_{TC}) can be calculated using the equation defined by Haacke, $\varphi_{TC} = \frac{T_{av}^{10}}{R_s}$, where R_s is the sheet resistance and T_{av} is average transmittance [19].

Fig. 5 demonstrates that the FOM value initially increase monotonically from 0 to 1% O_2/Ar gas flow ratio, until it attains the best value, and decrease as O_2/Ar flow ratio was 1.25. This change is a consequence of variation in transmittance. The overall the FOM represents over $20 \times 10^{-3}\ \Omega^{-1}$. From the plot, the multilayer film of SnO_2 (35 nm)/Ag (13 nm)/SnO_2 (35 nm) exhibits the best figure of merit with $35.3 \times 10^{-3}\ \Omega^{-1}$. Table 1 shows summarized data of the best figure of merit between the literature and the proposed structures for comparison. Considering the transmittance of substrates, it is obvious that conventional glass substrates show better performance than PET substrates. As compared with other multilayer film on PET substrate, the FOM result indicate that SnO_2 (35 nm)/Ag (13 nm)/

Table 1. Comparison of the best figure of merit between the literature and proposed structures.

Ref	Process method	SnO_2/Ag/SnO_2 Thickness (nm)	Highest figure of merit ($\times 10^{-3}\ \Omega^{-1}$)	Substrate
20	Magnetron Sputtering	25/5/25	16	glass
21	Magnetron Sputtering	25/10/25	33.9	glass
22	E-beam evaporation	45/10/45	13.3	glass
23	Magnetron Sputtering	30/10/30	21.32	PET
This study	Magnetron Sputtering	35/13/35	35.3	PET

SnO_2 (35 nm) multilayer thin film on PET shows similar worthy performance and a promising candidate for future flexible application.

Conclusions

In summary, we investigated the structural, optical, electrical properties of SnO_2 (35 nm)/Ag (13 nm)/SnO_2 (35 nm) multilayer thin films deposited at various O_2/Ar gas flow ratio. XRD pattern shows multilayers are amorphous. Overall transmittance increased with increase O_2/Ar flow ratio. Resistivity and sheet resistance almost remained at $6.0 \times 10^{-5}\,\Omega$·m and $7.5\,\Omega/\square$. The highest value of figure of merit is $35.3 \times 10^{-3}\,\Omega^{-1}$ for SnO_2 (35 nm)/Ag (13 nm)/SnO_2 (35 nm) multilayer, while the optical transmittance is 87.1% at 550 nm, the resistivity is $5.9 \times 10^{-5}\,\Omega$·cm, and sheet resistance is $7.1\,\Omega/\square$. The results of this study show that SnO_2/Ag/SnO_2 multilayer thin films have a high figure of merit improvement with 1% O_2/Ar gas flow ratio, which are promising candidates for the optoelectronic applications.

Acknowledgments

This work was supported by the Industrial Technology Innovation Program funded by the Ministry of Trade, Industry and Energy (MOTIE, Korea) (No. 10040000-10048659).

References

1. D.S. Hecht, L.B. Hu, G. Irvin, Adv. Mater. 23 (2011) 1482-1513.
2. Y. Shigesato, R. Koshi-ishi, T. Kawashima, J. Ohsako, Vacuum 59 (2000) 614-621.
3. Y. Leterrier, L. Medico, F. Demarco, J.-A.E. Manson, U. Betz, M. F. Escola, M. Kharrazi Olsson, F. Atamny, Thin Solid Films 460 (2004) 156-166.
4. S.X. Zhang, S. Dhar, W. Yu, H. Xu, S.B Ogale, and T. Venkatesan, J. Appl. Phys. 91(2007) 112113.
5. U. Ozgur, Y.I. Alivov, and C. Liu, J. Appl. Phys. 98 (2005) 041301.
6. A.N. Banerjeea, C.K. Ghosha, and K.K. Chattopadhyaya, Thin Solid Films 496[1] (2006) 112-116.
7. J.C. Hwang, M.C. Choi, and Y. Ha, Journal of Nanoscience and Nanotechnology 11 (2011) 550-554.
8. N. Zhou, D.B. Buchholz, G. Zhu, X. Yu, H. Lin, A. Facchetti, T.J. Marks, R.P.H. Chang, Adv. Mater. 26[7] (2014) 1098-1104.
9. K. L. Chopra, S. K. Major, and D. K. Pandya, Thin Solid Films 102, 1 (1983) 1-46.
10. H. Han, N.D. Theodore, and T.L. Alford, J. Appl. Phys. 103 (2008) 013708.
11. A. Dhar and T.L. Alford, J. Appl. Phys. 112 (2012) 103113.
12. J.G. Kim, S.M. Yoon and G.E. Jang, Journal of Ceramic Processing Research 17 (2016) 80-84.
13. J.G. Kim and G.E. Jang, Journal of Ceramic Processing Research 17 (2016) 103-108.
14. Y. Cho, N.S. Parmar, S. Nahm, and J.W. Choi, Ceramics International 43 (2017) 7216-7221.
15. S.M. Yoon and G.E Jang, Journal of Nanoscience and Nanotechnology 13 (2017) 7756-7759.
16. J. H. Kim, Y. J. Moon, S. K. Kim, Y. Z. Yoo and T. Y. Seong, Ceramics International. 41, 10(2015) 14805-14810.
17. S.Li, X. Qiao, J. Chen, Materials Chemistry and Physics 98 (2006)144-147.
18. I. Hanmberg, C.G. Granqvist, J. Appl. Phys. 60 (1986) R123.
19. G. Haacke, J. Appl. Phys. 47 (1976) 4086-4089.
20. S.H Yu, C.H. Jia, H.W. Zheng, L.H. Ding and W.F. Zhang, Materials Letters 85 (2012) 68-70.
21. L. Liu, S. Ma, H. Wu, B. Zhu, H. Yang, J. Tang and X. Zhao, Materials Letters 149 (2015) 43-46.
22. A. Bou, P. Torchio, D. Barakel, F. Thierry, P.Y. Thoulon and M. Ricci, Proc. Of SPIE. 8987 (2014) 898706.
23. T.K Kim and G.E Jang, Journal of Nanoelectronics and Optoelectronics (12) 2017 881-885.